A mutli-technique search for the most primitive CO chondrites

Journal Item

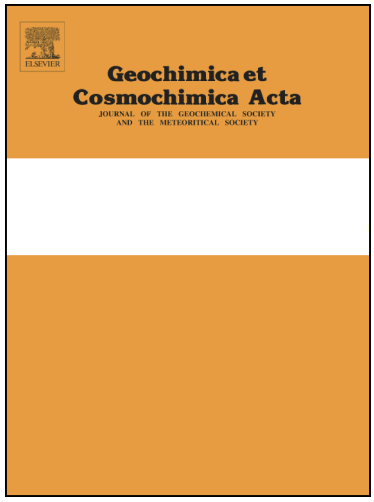

A mutli-technique search for the most primitive co chondrites

C.M.O'D. Alexander, R.C. Greenwood, R. Bowden, J.M. Gibson, K.T. Howard, I.A. Franchi

PII: S0016-7037(17)30244-2
DOI: http://dx.doi.org/10.1016/j.gca.2017.04.021
Reference: GCA 10246

To appear in: *Geochimica et Cosmochimica Acta*

Received Date: 9 December 2016
Accepted Date: 14 April 2017

Please cite this article as: Alexander, C.M.OaposD., Greenwood, R.C., Bowden, R., Gibson, J.M., Howard, K.T., Franchi, I.A., A mutli-technique search for the most primitive co chondrites, *Geochimica et Cosmochimica Acta* (2017), doi: http://dx.doi.org/10.1016/j.gca.2017.04.021

A MUTLI-TECHNIQUE SEARCH FOR THE MOST PRIMITIVE CO CHONDRITES.

C.M.O'D. Alexander, Dept. Terrestrial Magnetism, Carnegie Institution of Washington, 5241 Broad Branch Road, NW, Washington DC 20015, USA (calexander@carnegiescience.edu). Correspondence author.

R.C. Greenwood, Planetary and Space Sciences, Department of Physical Sciences, The Open University, Walton Hall, Milton Keynes, MK7 6AA, UK.

R. Bowden, Geophysical Laboratory, Carnegie Institution of Washington, 5251 Broad Branch Road, NW, Washington DC 20015, USA.

J.M. Gibson, Planetary and Space Sciences, Department of Physical Sciences, The Open University, Walton Hall, Milton Keynes, MK7 6AA, UK.

K.T. Howard, Physical Sciences Department, Kingsborough Community College, City University of New York, 2001 Oriental Blvd., Brooklyn, New York, NY 11235, USA.

I.A. Franchi, Planetary and Space Sciences, Department of Physical Sciences, The Open University, Walton Hall, Milton Keynes, MK7 6AA, UK.

Abstract

As part of a study to identify the most primitive COs and to look for weakly altered CMs amongst the COs, we have conducted a multi-technique study of 16 Antarctic meteorites that had been classified as primitive COs. For this study, we have determined: (1) the bulk H, C and N abundances and isotopes, (2) bulk O isotopic compositions, (3) bulk modal mineralogies, and (4) for some selected samples the abundances and compositions of their insoluble organic matter (IOM). Two of the 16 meteorites do appear to be CMs – BUC 10943 seems to be a fairly typical CM, while MIL 090073 has probably been heated. Of the COs, DOM 08006 appears to be the most primitive CO identified to date and is quite distinct from the other members of its pairing group. The other COs fall into two groups that are less primitive than DOM 08006 and ALH 77307, the previously most primitive CO. The first group is composed of members of the DOM 08004 pairing group, except DOM 08006. The second group is composed of meteorites belonging to the MIL 03377 and MIL 07099 pairing groups. These two pairing groups should probably be combined. There is a dichotomy in the bulk O isotopes between the primitive (all Antarctic finds) and the more metamorphosed COs (mostly falls). This dichotomy can only partly be explained by the terrestrial weathering experienced by the primitive Antarctic samples. It seems that the more equilibrated samples interacted to a greater extent with ^{16}O-poor material, probably water, than the more primitive meteorites.

Introduction

Primitive COs are of considerable interest for a number of reasons. For instance, they can preserve in their matrices some of the highest abundances of presolar silicates observed in any chondrites (Nguyen et al., 2007; Nguyen et al., 2010). This is presumably because they experienced low degrees of both metamorphism and aqueous alteration. The study of the most primitive matrices in chondrites, including in COs, will help determine how variable matrix is between chondrite groups, and how closely related it is to IDPs and cometary material, such as that from comet Wild 2. Metamorphism and aqueous alteration may have modified chondrule components, particularly glass compositions, complicating the interpretation of the apparent Al-Mg chondrule ages (Alexander, 2005; Alexander and Ebel, 2012). Identification of the most primitive COs will minimize the possibility that the internal isotope systematics of chondrules have been disturbed, although care will still have to be taken to only select the most pristine chondrules (e.g., Ushikubo et al., 2013). Ungrouped meteorites, such as Acfer 094, that have many affinities to the COs, also contain high abundances of presolar grains (Nguyen and Zinner, 2004; Vollmer et al., 2009), as well as unusual components, such as the so-called cosmic symplectite (Sakamoto et al., 2007; Seto et al., 2008) that may hold clues to the origin of water and non-solar O isotopes in the inner Solar System. The discovery of very primitive COs would also help to determine whether the COs and other chondrite groups accreted insoluble organic matter (IOM) that was similar to the IOM in CRs (Alexander et al., 2007), or whether the IOM accreted by each chondrite group varied as a result of changing nebular conditions. Finally, it is possible that relatively unaltered CMs like Paris (Hewins et al., 2014) that contain abundant metal could have been misclassified as COs.

As well as being of interest in its own right, IOM is a sensitive indicator of metamorphism, with IOM becoming less abundant and more ‘graphitic’ with increasing metamorphism (Quirico et al., 2003; Alexander et al., 2007; Bonal et al., 2007; Busemann et al., 2007; Cody et al., 2008). Since IOM is the major C-bearing component of chondrites and the C isotopic composition of IOM tends to also change during metamorphism, bulk C abundances and isotopic compositions may be useful preliminary

indicators of petrologic type. Similarly, bulk H abundances and isotopes can be useful indicators of the degree of aqueous alteration (Alexander et al., 2013). Bulk C and H abundances and isotopes in a suite of COs were used to identify DOM 08006 as a potentially very primitive CO3 (Alexander et al., 2014). A subsequent presolar grain search showed that it has the highest matrix-normalized presolar silicate abundance of any chondrite (Nittler et al., 2013). Position sensitive detector X-ray diffraction (PSD-XRD) has proven to be a very useful tool both for determining bulk mineral abundances and for classification (Bland et al., 2004; Menzies et al., 2005; Dunn et al., 2010; Howard et al., 2010, 2011; Howard et al., 2015). Lastly, bulk O isotopes are an indispensable tool for classifying meteorites and for providing constraints on the influence of fluids during parent body processing (e.g., Clayton and Mayeda, 1999; Young et al., 1999; Greenwood and Franchi, 2004; Schrader et al., 2011).

Here, we report the results of an initial search for very primitive COs and minimally altered CMs amongst 16 Antarctic meteorites whose preliminary classifications indicated that they were low petrologic type COs. This study uses bulk analytical methods (bulk H, C, N, and O isotopes) combined with bulk PSD-XRD and analyses of isolated IOM both to classify these COs and to identify the most primitive ones among them.

Methods

0.5-3g samples were acquired of 16 relatively large Antarctic meteorites whose preliminary classification suggested that they are primitive CO3s (Table 1). The samples were crushed to a grain size of <150 μm. Aliquots were then analyzed for their bulk H, C and N abundances and isotopic compositions (Table 1, Fig. 1). Subsets of the samples were subsequently analyzed for the abundances and isotopic compositions of H, C and N in their IOM (Table 2), for their bulk O isotopic compositions (Table 3) and for their bulk mineralogy by PSD-XRD (Table 4).

IOM isolation

The new IOM residues were prepared and analyzed using the same methods as described in Alexander et al. (2007). The new residues were prepared using the CsF-HF

technique in which crushed samples (<106 μm) are first leached with 2N HCl, followed by rinsing with milliQ water and dioxane, and then shaken in the presence of two immiscible liquids, a CsF-HF solution (1.6-1.7 g/cc) and dioaxane. When liberated from the mineral matrix, the IOM collects at the interface of the CsF-HF solution and the dioxane, while the denser minerals sink to the bottom. After centrifugation, the IOM is pipetted off and rinsed with 2N HCl, milliQ water and then dioxane, before being dried down at <30-50°C. There was no specific attempt to remove soluble organic material. However, the repeated washing with aqueous solutions and dioxane should have effectively removed most soluble organic compounds known to be present in chondrites.

H, C and N analyses

For the elemental/isotopic analyses, aliquots of the meteorite powders were weighed into foil capsules (Ag for H, Sn for C and N) and were stored in desiccators for days to weeks at room temperature to minimize adsorbed water contents. However, this process will not have removed all of the terrestrial water associated with weathering products. The samples were weighed prior to being placed in the desiccators and again several days later. Typical sample weights were 5-6 mg for bulk H measurements, 8-9 mg for bulk C and N measurements, and 0.3 mg of IOM for both the H and the C and N measurements. Weight losses after desiccation ranged from 0.3 wt.% to 3 wt.%. The highest weight losses were for Buckley Island (BUC) 10943 and Miller Range (MIL) 090073, both of which it turns out are probably CMs.

Elemental and isotopic analyses were made with: 1) a Thermo Scientific DeltaV^{plus} mass spectrometer connected to a Carlo Erba (NA 2500) elemental analyzer (CE/EA) via a Conflo III interface for C and N analyses, and 2) a Thermo Finnigan Delta^{plus}XL mass spectrometer connected to a Thermo Finnigan Thermal Conversion elemental analyzer (TC/EA) via a Conflo III interface for H analyses. The Conflo III interface facilitates the introduction of the N_2 and CO_2 reference gases for the N and C isotope analyses, while a dual inlet system facilitates introduction of the D/H reference gas for the H isotope analyses. A H_3^+ correction was determined and applied to the H measurements. We used in house standards to normalize and correct the data at regular intervals (e.g., every 10-12

samples) to monitor the accuracy and precision of the measured isotopic ratios and elemental compositions throughout the runs. These in house standards, which included both gases and solid materials, have been calibrated against international (SMOW, NBS-22, PDB and air) and other certified standards from Isoanalytical, USGS, NBS and Oztech.

For H analyses, two samples of each meteorite were analyzed sequentially to check for both sample heterogeneity and small memory effects that are known to occur with D enriched samples. Blanks were run between different meteorites, again to reduce any memory effects. There was little evidence for significant heterogeneity or memory effects. For example, the H abundances of the duplicate samples generally differed by ≤1 % of their absolute values, and the δD values differed by 0.1-3.8 ‰ (the δ notation stands for the deviation of a sample ratio from a standard ratio in parts per thousand, $\delta=(R_{smp}/R_{std}-1)*1000$ and in this case R=D/H). There is no memory effect for C and N analyses, and the larger sample sizes ensured more representative sampling of the powders. Generally, only one sample of each meteorite was analyzed for C and N. Past experience (Alexander et al., 2012; Alexander et al., 2013) indicates that C and N abundances typically vary by 1-5 % of their absolute values, $\delta^{13}C$ values varied by 0.1-0.7 ‰, and $\delta^{15}N$ values varied by 0.1-1 ‰. Differences in composition between different chips of the same meteorite can be larger than these analytical uncertainties, as illustrated by the results in Table 1, suggesting that meteorite heterogeneity is the major source of uncertainty.

Oxygen isotope analyses

Oxygen isotopic analyses were undertaken at the Open University using an infrared laser-assisted fluorination system (Miller et al., 1999). The normal operating procedure involves loading 0.5-2 mg aliquots of samples and standards into a Ni sample block containing 22 drilled wells. The sample block is then loaded into a two-part chamber, made vacuum tight using a compression seal with a Cu gasket and quick-release KFX clamp (Miller et al., 1999). For samples with a large fraction of hydrous phases, it is generally better not to load multiple aliquots into a single tray (Schrader et al., 2014). This is because selective removal of such phases can take place as a result of repeated

exposure to BrF_5 even at room temperature. However, the low hydrated mineral contents of COs mean that it is perfectly acceptable to run multiple aliquots in a single tray. Throughout the course of this study, there was no evidence of isotopic shifts that could be accounted for by pre-reaction.

A 3 mm thick BaF_2 window at the top of the chamber allows simultaneous viewing and laser heating of samples. Sample heating in the presence of BrF_5 is carried out using an integrated 50 W infrared CO_2 laser (10.6 μm) and video system mounted on an X-Y-Z gantry supplied by Photon Machines Inc. After fluorination, the O_2 released is purified by passing it through two cryogenic N_2 traps and over a bed of heated KBr. The isotopic composition of the purified O gas is then analyzed using a Thermo Fisher MAT 253 dual inlet mass spectrometer (mass resolving power ~200). Analytical precision (1σ) for the system, based on replicate analyses of an internal obsidian standard (n=39) is: ±0.025 ‰ for $\delta^{17}O$; ±0.045 ‰ for $\delta^{18}O$; ±0.01 ‰ for $\Delta^{17}O$ (Starkey et al., 2016).

Interference at m/z=33 by NF^+ was monitored by performing scans for NF_2^+. Traces of NF_2^+ were detected in a small subset of runs undertaken as part of this study. Individual replicates were rejected where the monitored NF_2^+ peak was greater than 1 mV. Operational experience has demonstrated that below this level interference from NF^+ is negligible.

As demonstrated by Greenwood and Franchi (2004), significant shifts in the O isotope composition of Antarctic COs can occur as a consequence of terrestrial weathering. In order, to evaluate the extent of this problem, a subset of primitive COs were leached in a solution of ethanolamine thioglycollate (EATG), which has proved to be efficient at removing terrestrial weathering products from a range of meteorite types, without significantly disturbing their primary O isotope composition (Greenwood et al., 2012).

The precision (1σ) quoted for individual samples is based on replicate analyses. Oxygen isotopic analyses are reported in standard δ notation, where $\delta^{18}O$ has been calculated as: $\delta^{18}O = [(^{18}O/^{16}O_{sample})/(^{18}O/^{16}O_{ref})-1] \times 1000$ (‰) and similarly for $\delta^{17}O$ using the $^{17}O/^{16}O$ ratio. $\Delta^{17}O$, which represents the deviation from the terrestrial fractionation line, has been calculated as: $\Delta^{17}O = \delta^{17}O - 0.52 \times \delta^{18}O$. Isotopic compositions are relative to Vienna Standard Mean Ocean Water (VSMOW).

Position sensitive detector X-ray diffraction

0.1-0.15 g aliquots of the larger powdered samples that were prepared for bulk H, C, N and O isotopic measurements were gently ground by hand in an agate mortar and pestle to finer powders, with no grains or clumps greater than 35 µm. Roughly 100 mg of these finer powders were packed in circular Al wells using the sharp edge of a spatula. This preparation minimizes the tendency for preferred alignment of platy minerals and allows us to collect random powder diffraction patterns that are representative of the bulk powder.

The PSD-XRD analyses used a Nonius PDS 120 powder diffraction system consisting of an INEL curved PSD within a static beam-sample geometry. A Ge monochromator in the primary beam selects only Cu Kα radiation, horizontal and vertical slits define the beam size at the sample, and diffracted X-rays are detected simultaneously around 120° of arc by the PSD. The ability to collect data simultaneously over 120° of diffraction allows for whole pattern profiling, which is important when de-convolving the mineralogy of fine grained and complex polyphase samples. This instrumentation overcomes the effects of preferred orientation and non-constant sample-area irradiation that make the task of phase quantification by conventional scanning diffractometry extremely difficult. A fluorescent powder that was prepared identically to the studied samples was analyzed to image the beam and ensure that it was entirely absorbed by powder and does not hit the sample holder; the size of the incident beam was approximately to 0.24 x 2.00 mm. The incident angle that the beam strikes the sample was set to roughly 3.6° so as to resolve low angle diffraction that is critical for identifying phyllosilicates. Diffraction patterns for the powdered meteorite samples were collected for up to 16-22 hours so as to maximize the signal-to-noise ratios in the resulting patterns.

The first step of quantification of the XRD patterns is the identification of the phases present using the ICCD database. Once phases are identified in the meteorite samples, we select examples of these minerals from the collections at The Natural History Museum (London), American Museum of Natural History (New York) and Smithsonian National Museum of Natural History (Washington D.C.) to be used as standards in pattern fitting

following the method of Cressey and Schofield (1996). The PSD-XRD array has a fixed geometry and the selected minerals were analyzed immediately after the meteorite in the same lab session, in the same sample holder and under the same the flux of X-rays (flux is monitored throughout the measurements), therefore analytical conditions were identical for the meteorite and the mineral standards. Collection times for the meteorites and standards were normalized for quantification. The diffraction pattern for an identified standard (100 % single phase) is reduced in intensity by a proportion/pattern fit factor to produce a best-fit match to its intensity in the mixture pattern and is subtracted to leave a residual. When the sum of the pattern fit proportions equals 1 and a peak-free residual of zero counts is reached all phases in the mixture are accounted for. The pattern fit proportions are corrected for their relative differences in X-ray absorption to yield modal abundances in wt.% that are usually converted to vol.% using known phase densities. This pattern fitting approach is accurate to within 1–3 vol.% as demonstrated in international round robins that tested the phase quantification of blind mixtures (Madsen et al., 2001). Application of this technique to meteorites has been described in numerous publications where errors are shown to be 1–3 vol.% for anhydrous phases and 2–4 vol.% for phyllosilicates (Bland et al., 2004; Menzies et al., 2005; Dunn et al., 2010; Howard et al., 2010, 2011; Howard et al., 2015; King et al., 2015).

Despite producing intrinsically noisier diffraction data than some other wavelengths, the advantage of using Cu-radiation is that it induces fluorescence on interaction with Fe-bearing materials, the intensity of the fluorescence from a sample being proportional to its Fe content. This makes it possible to identify Fe-rich amorphous material, its signature being revealed in residual X-ray counts after the crystalline components have been subtracted from the bulk patterns during pattern fitting. The counts from X-ray amorphous material appear as ‘hump’ like features in the residual patterns, the shapes of which are not truly diagnostic of the phase(s) identity. We therefore quantify only the total contribution of Fe-bearing X-ray amorphous material in the samples, but cannot resolve the specific contributions of phases known to be amorphous in carbonaceous chondrites (e.g., Fe-bearing silicates and Fe-oxides/hydroxides). Previously, we have used carbonaceous chondrite bulk compositions and petrography to demonstrate that most amorphous material in primitive carbonaceous chondrites is Fe-rich silicate in

matrix (e.g., Howard et al., 2015).

Results

Carbon, hydrogen and nitrogen abundances and isotopes

The range of bulk C contents and isotopic compositions is considerable (Table 1). Most of the meteorites appear to fall into two groups (Groups 1 and 2) that are not entirely consistent with their nominal pairings (Table 1).

The bulk H abundances and δD values also exhibit a considerable spread (Table 1 and Fig. 1). Most of the meteorites cluster in a single group (H=0.3-0.4 wt.%, δD=-80 ‰ to -90 ‰), but there is a linear trend to higher H contents and lighter isotopic compositions that is most obvious in the two most weathered meteorites, MIL 03442 and MIL 090785, and in MIL 090073. The two Dominion Range (DOM) 08006 samples and Allan Hills (ALH) 77307 have the highest bulk δD values of any of the COs measured here. They appear to form a second trend that intersects the first at roughly the bulk composition of the most weathered sample, MIL 090785.

IOM abundances and H, C, and N compositions have been determined for a subset of the COs (Table 2). The upper ranges of H/C ratios and δD values are higher than previously reported for COs (Alexander et al., 2010).

Oxygen isotopes

The O isotope compositions for 13 of the 16 Antarctic COs included in this study are given in Table 3 and plotted in Figure 2. The six CO falls also analyzed as part of this study (Table 3 and Fig. 2) are: Kainsaz (3.2/3.6), Felix (3.3/3.6), Ornans (3.4/3.6), Moss (3.4-3.5), Lancé (3.5/3.6), Warrenton (3.7) - the petrologic types are from Chizmadia et al. (2002) and Bonal et al. (2007), respectively, except for Moss which is from Greenwood et al. (2007). MIL 090073 was previously classified as a CO3, but it is clear from its O isotope composition (Table 3) that it is a CM. The CO falls define a relatively restricted field that plots on the carbonaceous chondrite anhydrous mineral (CCAM) line

(Fig. 2). Compared to the previous CO fall data of Greenwood and Franchi (2004), our new fall analyses show a slight shift towards the CCAM line. The reasons for this shift are unclear, but may reflect incomplete fluorination in the case of the Greenwood and Franchi (2004) results that were obtained using an earlier generation of laser and beam delivery system. However, both sets of data are essentially within error of each other. With the exception of the primitive COs ALH 77307 and Colony, the Antarctic and non-Antarctic finds that were previously measured by Greenwood and Franchi (2004) have compositions that are close to the new CO fall analyses (Fig. 2).

Compared to the CO falls, the untreated primitive Antarctic COs analyzed in this study are displaced to lighter isotopic compositions and, with the notable exception of MIL 090785, define a relatively restricted linear field in Figure 2 that is distinct from the compositions of the more equilibrated COs. The best fit line ($\delta^{17}O = -4.84 + 0.52\times\delta^{18}O$, $R^2 = 0.95$) through the primitive COs (excluding MIL 090785) and the more equilibrated falls (Fig. 2) has a slope that is essentially identical to that of a mass fractionation line, suggesting that perhaps primitive COs have distinct O isotopic compositions from the more equilibrated members of their group. However, as noted by Greenwood and Franchi (2004), Antarctic CO finds have experienced variable degrees of terrestrial alteration, and the primitive COs also plot close to a mixing trend between the CO falls and SLAP (Standard Light Antarctic Precipitation). This line is shown by the grey arrow in Figure 2 and has the following formula: $\delta^{17}O = -5.04 + 0.43\times\delta^{18}O$ $R^2 = 1.00$.

In order to mitigate the potential effects of Antarctic weathering, a subset of 7 of our primitive CO samples were leached in EATG (Table 3, Fig. 2). In addition, three CO samples that were studied previously by Greenwood and Franchi (2004) (ALH 77307, ALH 82101, Colony) were also leached in EATG. Compared to the untreated samples, the EATG-leached primitive Antarctic COs exhibit marked shifts towards the CCAM line in Figure 2. This behavior is also seen in the EATG residues for ALH 77307 and ALH 82101, and to a lesser extent for the non-Antarctic find Colony (Fig. 2). The overall shift for a number of the samples appears to be greater with respect to $\delta^{17}O$ than $\delta^{18}O$, as is clearly the case for Colony (Fig. 2). The most notable exception to this is MIL 090785, the most weathered sample, which shows a large change in $\delta^{18}O$.

ALH 77307, which is known to be amongst the most primitive of COs (Brearley, 1993; Chizmadia et al., 2002; Grossman and Brearley, 2005; Bonal et al., 2007), shifts close to the other primitive COs following EATG treatment (Fig. 2). In contrast, the EATG residue for ALH 82101 is displaced towards the CO falls. This may be a reflection of its higher metamorphic grade, which is estimated to be 3.3 compared to 3.0 for ALH 77307 (Greenwood and Franchi, 2004). The EATG residue for the non-Antarctic primitive CO find Colony is displaced in the direction of the CO falls compared to its untreated bulk analysis. The fact that the EATG residue for Colony is somewhat displaced from the CCAM may indicate that leaching did not remove all of the secondary minerals from this heavily weathered find. MIL 090785 displays a very large isotopic shift following EATG treatment, with its residue plotting well to the right of the CCAM line (Fig. 2). It is unclear why MIL 090785 displays such a large $\delta^{18}O$ shift after EATG treatment, but this is presumably a reflection of its extremely weathered composition.

The aim of the EATG treatment was to selectively remove terrestrial weathering products, with minimal loss of primary constituents. To verify whether or not EATG treatment can cause significant shifts in the primary O isotope compositions of the COs, three CO falls (Lance, Ornans and Warrenton) were also leached in EATG at room temperature under the same conditions and using the same procedures as for the Antarctic COs. The EATG treatments of the falls (Table 3, Fig. 3) resulted in small shifts in the O isotopic compositions of all three samples compared to their untreated compositions, with the untreated samples being isotopically heavier than the leached ones. The magnitude of this shift in $\delta^{18}O$ ranges from ~0.5 ‰ in the case of Lance to about 0.9 ‰ for both Ornans and Warrenton. The leached falls are not significantly shifted away from the CCAM line suggesting that the phase being removed during treatment is an isotopically heavy component that plots on or close to the CCAM. Amorphous materials in the matrix and in chondrule mesostases are two potential candidates for the leached material.

A more detailed analysis of the effects of Antarctic weathering on the primary O isotope composition of COs is given in the discussion section.

Modal mineralogies

The PSD-XRD results (Table 4) show that all of the primitive Antarctic COs are dominated by olivine and pyroxene, but that they also contain abundant amorphous material (23-37 vol.%) and very low abundances of poorly crystalline phyllosilicates (0-3 vol.%). Given the low bulk H contents of these samples, the amorphous material is unlikely to be dominated by FeOH and if the amorphous signature was from sulfide, bulk S contents would be far greater than measured in COs. We therefore interpret the bulk of the amorphous component in these samples to be Fe-bearing silicate. Neither the abundances of amorphous material or the phyllosilicates in the COs appear to correlate with light element abundances or weathering grade. BUC 10943 (Table 4) is distinct from the other samples in that it contains roughly equal abundances of cronstedtite and serpentine that together total ~70 vol.%. This meteorite is most likely a CM rather than a CO.

Discussion

Classification and pairing

Two of the 16 meteorites studied appear to be CMs. For BUC 10943, the H, C and N bulk (Table 1) and IOM (Table 2) isotopic compositions, as well as the PSD-XRD results (Table 4), point to it being a typical CM with a petrologic type of 1.4 on the scale of Alexander et al. (2013). However, the bulk C content of BUC 10943 is low for a CM, and its IOM yield even lower. MIL 090073 has bulk O isotopes that suggest it is also a CM (Table 3). If it is a CM, its low bulk H and C contents and intermediate H isotopic composition (Table 1), compared to most CMs (Alexander et al., 2012; Alexander et al., 2013), suggest that it might have been heated. This would be consistent with the absence of resolvable diffraction from phyllosilicates in its PSD-XRD patterns. The H/C ratio of IOM can also be used as an indicator of heating, but unfortunately the IOM H measurement for MIL 090073 failed and there was insufficient material to attempt a new measurement. Brief examination of one thin section of MIL 090073 (MIL 090073,2) found that matrix and chondrule abundances are consistent with a CM chondrite, as is the almost complete absence of metal. However, in most of the section the matrix contains numerous cracks, some of which are filled with Ca-sulfate, and little or no cronstedtite, sulfide or tochilinite. In one region of the section, the matrix does contain abundant

intergrown cronstedtite/sulfide and isolated sulfide grains, but no tochilinite was observed. There seems to be a gradation rather than a sharp boundary between the cronstedtite-bearing and cronstedtite-free regions. MIL 090073 does seem to be a CM, but heating and weathering (e.g., Ca-sulfate filled cracks) may have contributed to its low phyllosilicate and C contents. These two CMs will not be discussed further in this paper.

The remaining COs have been subdivided based on their bulk C abundances and isotopic compositions (Table 1). The variation in bulk C content probably reflects variations in matrix abundance and/or petrologic type – both decreasing matrix abundance and increasing thermal metamorphism will lead to lower bulk C contents.

The high C content of DOM 08006, even compared to ALH 77307, sets it apart from all of the other COs, including members of its nominal pairing group. The high yield and composition of the IOM in DOM 08006 confirms its unique status (Table 2). There is no indication that DOM 08006 has ~50 % more matrix than ALH 77307 as the difference in their bulk C contents would require. Thus, the high bulk C abundance of DOM 08006 suggests that it less metamorphosed than ALH 77307 and that it is the most primitive CO yet identified. That DOM 08006 is more primitive than ALH 77307 is also consistent with the higher presolar silicate abundance of DOM 08006 matrix (Nittler et al., 2013) and its lower petrologic type based on the Cr contents of its olivine (Davidson et al., 2014a). The higher H/C ratio of its IOM (Table 2) is also indicative of the more primitive nature of DOM 08006 compared to ALH 77307. The similarity in IOM H/C ratios between DOM 08006 and Semarkona (LL3.00) (Table 2) suggests that they experienced similar thermal histories and, therefore, DOM 08006 is also petrologic type 3.00. Bonal et al. (2007) suggested that ALH 77307is a type 3.03, which is consistent with our results. However, there is a dramatic difference in their bulk IOM δD values (DOM 08006<<Semarkona), indicating that they either had somewhat different IOM precursors, or that parameters other than temperature determined the evolution of bulk IOM δD values during parent body processing (e.g., Alexander et al., 2010).

While DOM 08006 may not be part of the DOM 08004 pairing group, DOM 10104 and DOM 03238 do seem to be very similar to DOM 08004 in terms of their bulk C abundances and isotopes (Table 1). These three meteorites constitute our Group 1. DOM 03238 is not officially part of the DOM 08004 pairing group, but our data suggests that it

should be. Olivine Cr measurements for DOM 10104 suggest that it has a higher petrologic type than ALH 77307 despite its higher bulk C content (Davidson et al., 2014a). Consequently the ~5-8 % difference in C contents between ALH 77307 and the three meteorites in Group 1 is probably due to variations in matrix contents. This illustrates that bulk C content alone is not always a reliable petrologic indicator.

All but two of the remaining COs analyzed here have very similar bulk C abundances and isotopes, and they have been assigned to Group 2. All of these meteorites belong to the MIL 03377 and MIL 07099 pairing groups. The fact that all these meteorites are so similar suggests that the MIL 03377 and MIL 07099 pairing groups should be combined. Olivine Cr measurements for MIL 05024 and MIL 090010 indicate that they have slightly higher petrologic types than the Group 1 meteorite DOM 10104 (Davidson et al., 2014a), which is consistent with their lower bulk C contents and the lower bulk H/C ratios of their IOM. Based on the olivine Cr data, the Group 2 meteorites have lower petrologic types than any of the falls measured here for their O isotopes.

The two meteorites from the MIL 03377 and MIL 07099 pairing groups that have very different bulk C abundances and isotopes, MIL 03442 and MIL 090785, are weathering grade C. Both meteorites have lower C contents than the other members of the two pairing groups. The bulk C content of MIL 090785 is similar to that of Isna (petrologic type ~3.7). To determine whether MIL 090785 was heavily metamorphosed like Isna, we measured 36 relatively fayalitic (Fa18-53) olivine phenocrysts in chondrules (one per chondrule) and isolated grains in the matrix of one thin section (MIL 0900785,2). The mean and standard deviation of the grains Cr_2O_3 contents (0.30±0.15 wt.%) indicate that MIL 090785 is petrologically closer to Colony than its nominal pairing group member MIL 090010 (Davidson et al., 2014b). Nor does it seem to have an unusually low matrix content. Thus, weathering seems the most likely explanation for the low C content of MIL 090785, and by implication for MIL 03377. However, if weathering was the cause of their lower C contents, it would suggest a different mechanism of weathering compared to Antarctic CMs (except perhaps MIL 090073) and CRs as weathering does not seem to have influenced their C contents (Alexander et al., 2012).

Effects of weathering

As can be seen in Figure 1, the variation in the bulk H abundances and isotopic compositions of most of the COs suggest two component mixing, with one component being ~0.3 wt.% H and δD≈-80 ‰ and another whose composition is probably similar to, or more extreme than, MIL 090785. The MIL 090785-like component is most likely a terrestrial weathering product, while the isotopically heavier component is probably a mixture of indigenous organics and water of terrestrial and/or extraterrestrial origin.

The bulk O isotopic compositions of the untreated and EATG-treated primitive Antarctic COs can be explained in at least three ways. (1) Their pre-terrestrial bulk compositions were similar to those of the more equilibrated falls, but they weathered in the presence of water that had a highly fractionated, SLAP-like composition (SLAP: δD=-428 ‰, $\delta^{18}O$=-55.5 ‰) (Figs. 2 and 4). The shifts in $\Delta^{17}O$ towards the CCAM line after EATG treatment are the result of removal of an indigenous ^{16}O-poor material along with the weathering products (Figs. 2 and 4). The behavior of MIL 090785 after EATG treatment suggests that it is a more equilibrated CO. (2) The COs all initially contained a ^{16}O-poor component. This component is mass fractionated to lighter O isotopic compositions in the primitive COs and, unlike in the more equilibrated COs, is removed by the EATG. (3) All the primitive COs, except MIL 090785, interacted with water that was much less isotopically fractionated than typical Antarctic snow and ice, and there is a significant indigenous dichotomy in the bulk O isotopic compositions of primitive and more equilibrated COs.

Option 3 might be possible if the weathering products rapidly exchanged with atmospheric water during crushing and prior to O isotope analysis. Certainly, none of the meteorites, even the most weathered ones, have bulk H isotopic compositions that are close to that of SLAP. However, this explanation requires that the clustering of untreated primitive CO O isotopic compositions near the line connecting SLAP with the more equilibrated COs be a coincidence. Option 2 ignores the clear petrologic evidence and correlated H isotopic evidence that the primitive Antarctic COs all experienced some weathering. Weathering by a SLAP-like component would produce a range of O isotopic compositions that resemble a mass fractionation line (Figs. 2, 4). While at present we

cannot completely rule out Options 2 and 3, we believe that Option 1 is the most conservative and plausible explanation as it takes into account the clear evidence for Antarctic weathering in the most straightforward way. Hence, we explore it in more detail below.

In Figure 5, the CO falls, and untreated and EATG-treated primitive Antarctic finds analyzed in this study are plotted in relation to the SLAP standard. Weathering of meteorites in Antarctica results in the formation of a diverse mixture of secondary O-bearing phases, including oxides, oxyhydroxides, sulfates and a wide range of often poorly crystallized silicates (Lee and Bland, 2004; Hallis et al., 2014). Akaganeite (β-FeOOH), and smectite, two important secondary phases identified in Antarctic meteorites (Lee and Bland, 2004), serve to illustrate the O isotope shifts associated with cold desert secondary alteration (Fig. 5). Given a $\delta^{18}O$ composition for Antarctic "water" of -55.5 ‰ (SLAP) and an alteration temperature of close to 0°C, the $\delta^{18}O$ composition of akaganeite would be -53.3‰ (Bao and Koch, 1999; Beaudoin and Therrien, 2009). Under the same alteration conditions, smectite would have a $\delta^{18}O$ composition of -25.4 ‰ (Sheppard and Gilg, 1996; Beaudoin and Therrien, 2009). An alteration temperature close to 0°C is indicated by direct measurement of meteorite specimens in Antarctica (Schultz, 1986). While only two mineral compositions are plotted in Figure 5, these essentially define the likely range of secondary alteration products formed in Antarctic meteorites in equilibrium with meteoric waters with a composition close to SLAP. For instance, under the same alteration conditions serpentine would have a $\delta^{18}O$ composition of -29.4 ‰ (Zheng, 1993; Beaudoin and Therrien, 2009) and illite -27.7 ‰ (Savin and Lee, 1988; Beaudoin and Therrien, 2009). Thus, alteration by water with the composition of SLAP will form secondary minerals that plot along the terrestrial fractionation line (TFL) between the akaganeite and smectite end-members (Fig. 5).

In Figure 5, tie lines that join these secondary phases to Kainsaz (3.2/3.6), the least metamorphosed CO fall, intersect the field occupied by the untreated primitive Antarctic COs. This suggests that their isotopic compositions can be explained in terms of a primary composition that lies along the CCAM line, either overlapping or close to the field of CO falls, with subsequent Antarctic weathering shifting them in the direction of alteration products that plot on the terrestrial fractionation line (Fig. 5). MIL 090785 is

clearly the most altered primitive CO, which using the lever rule has approximately 24 % of its O derived from a SLAP-like source. In comparison, the other primitive COs have between 8 % and 13 % of their O derived from a SLAP-like source.

An additional complication is that analyses of surface snow samples in Antarctica indicate that they have highly variable isotopic compositions, with those analyzed by Yan et al. (2002) ranging from $\delta^{18}O$= -22.5 ‰ to -50.7 ‰. The average of these analyses is $\delta^{18}O$= -36.6 ‰ and so is somewhat less fractionated than SLAP. Alteration by water with this composition at a temperature of 0°C would result in the formation of akaganeite with a $\delta^{18}O$ composition of -34.4 ‰ (Bao and Koch, 1999; Beaudoin and Therrien, 2009) and smectite with a $\delta^{18}O$ composition of -6.5 ‰ (Sheppard and Gilg, 1996; Beaudoin and Therrien, 2009) (Fig. 6). Thus, alteration by meteoric waters with a less negative $\delta^{18}O$ composition than SLAP would have the effect of moving the secondary mineral assemblage to the right along the TFL (Fig. 6). The relationships seen in both Figures 5 and 6 are consistent with Antarctic alteration being the cause of the isotopic shift between the untreated primitive COs relative to the CO falls. Furthermore, the isotopic variability observed in the untreated primitive COs can potentially be explained by terrestrial alteration involving Antarctic meteoric waters having a similar range in $\delta^{18}O$ values to that measured by Yan et al. (2002) .

Based on the above analysis it would appear likely that prior to terrestrial alteration the primitive Antarctic COs had compositions that plotted on, or very close to, the CCAM line, and this possibility is strengthened by the results of the EATG leaching experiments (Fig. 2-4). The question that now arises is where on the CCAM line did the primitive Antarctic COs plot relative to the more equilibrated CO falls? As illustrated in Figures 5 and 6, the bulk compositions of the untreated primitive Antarctic samples are consistent with weathering of Kainsaz-like material. However, while the EATG leaching did move the samples toward the CCAM line it was not towards the more equilibrated CO compositions. Thus, unless the EATG leaching can also shift the residues along the CCAM line to lighter O isotopic compositions by several per mil, there still seems to be an O isotope dichotomy between the primitive and more equilibrated COs. The EATG leaching experiments on the more equilibrated COs (Fig. 3) did show that the treatment can lead to shifts in the residues of between -0.5 ‰ and -0.9 ‰ in $\delta^{18}O$ relative to the

untreated samples (Fig. 3). Yet even after shifting the primitive CO EATG-leached residues by +1 ‰ in $\delta^{18}O$ parallel to the CCAM line, the primitive Antarctic CO compositions would still be ^{16}O enriched compared to the more equilibrated CO falls. On the other hand, applying such a shift to the EATG residues would cause them to scatter about the composition of the anhydrous mineral separates from Murchison (Fig. 4). Clayton and Mayeda (1999) suggested that the anhydrous mineral separates represented the CM starting composition, and proposed that CO-like precursor materials were parental to the CMs. Our results are consistent with this possibility, although the CMs have higher matrix contents.

Water in the COs

IOM contributes 2-7 % of the H in the COs analyzed, with the highest contribution in DOM 08006. However, the isolated IOM does not account for the bulk C contents of the COs. Previously it has been shown that isolated IOM, soluble organic matter and carbonates cannot account for the bulk C contents of chondrites (Smith and Kaplan, 1970; Alexander et al., 2012; Alexander et al., 2015). The reason for this lack of mass balance may be because IOM-like material is lost, either as very fine particulates or as acid hydrolysable material, during IOM isolation. Even if one assumes that all the bulk C is in material with IOM-like H/C ratios, the IOM contribution to the bulk H is <10 %. This suggests that there is at least one additional H-bearing component in these meteorites, probably in phyllosilicates and/or amorphous material. The estimated bulk water/OH H contents and isotopic compositions are given in Table 5 for those meteorites whose IOM contents and compositions have been determined (Table 2). The estimated water content for ALH 77307 of 4.68 wt.% (0.52 wt.% H) is very similar to the measurement of 4.54 wt.% bound water in ALH 77307 reported by Jarosewich (1990). The bulk H content of DOM 08006 is much higher than for Semarkona (0.123 wt.%; Alexander et al., 2012). Yet, unlike in Semarkona, phyllosilicates were not found in DOM 08006 matrix (Davidson et al., 2014b), leaving hydrated amorphous material as the most likely additional H-bearing component. If correct, the primitive CO water contents are similar to those of the most primitive CRs (Alexander et al., 2013), which are also

thought to contain hydrated amorphous silicates with approximately 10 wt.% water/OH (Le Guillou and Brearley, 2014; Howard et al., 2015). The origin(s) of the water in the primitive COs has yet to be determined, but may have a combination of indigenous and terrestrial sources.

From the elemental composition determined by Jarosewich (1990), ALH 77307 contains 36.75 wt.% O, 4.04 wt.% of which is in bound water. Assuming a $\Delta^{17}O$=0 ‰ for this water and a $\Delta^{17}O$=-4.71 ‰ for the anhydrous material like that measured for Kainsaz by Greenwood and Franchi (2004), the bulk $\Delta^{17}O$=-4.19 ‰ and is very similar to the ALH 77307 bulk $\Delta^{17}O$=-4.12 ‰ (Greenwood and Franchi, 2004). Magnetite in chondrites is generally thought to form via oxidation of metal/sulfide by water. Assuming that there was no water-rock O isotopic exchange prior its formation, magnetite can be used to obtain a lower limit on the $\Delta^{17}O$ of the fluids that were present in a chondrite. The O isotopes have not been measured in magnetite from any of the COs studied here, but values of $\Delta^{17}O\approx$-2 ‰ have been reported for two other COs (Choi et al., 2008; Doyle et al., 2015). In principle, a $\Delta^{17}O$=0 ‰ for the bulk water could be the result of mixing between a component with a $\Delta^{17}O\approx$-2 ‰ and one that is isotopically much heavier, such as that responsible for producing the cosmic symplectite found in the CO-related Acfer 094 (Sakamoto et al., 2007). However, it is physically implausible that two separate water components could be maintained in a chondrite and that the ^{16}O-poorer component would contribute less to any magnetite formation. Thus, it is likely that most of the water in ALH 77307 is terrestrial. The estimated H isotopic composition of the water in ALH 77307 (Table 5) is not as fractionated as one would expect for Antarctic snow and ice, nor is it as fractionated as the more weathered COs. Either the fraction of organic H was underestimated in making the estimates in Table 5, or the water in ALH 77307 exchanged with water from lower latitudes with less fractioned H isotopic compositions than Antarctic snow/ice. The same would also be true for DOM 08006.

However, addition of terrestrial water to a Kainsaz-like precursor cannot explain the apparent dichotomy that appears to exist between the EATG-treated CO finds and the more equilibrated CO falls (e.g., Fig. 2). As demonstrated by leaching of the CO falls, in addition to terrestrial weathering products, EATG treatment probably removes a ^{16}O-poor primary component from the finds. This results in a slight shift of up to -1 ‰ parallel to

the CCAM line. This may indicate that the gap between the falls and EATG-treated finds is an artifact and that primary compositions would have formed a continuous array along the CCAM line, with the most primitive samples such as DOM 08006 (Fig. 4) plotting at the ^{16}O-rich end, whereas the more equilibrated samples plot at the ^{16}O-poor end. Such a distribution requires some form of exchange between a primitive ^{16}O-rich end member (DOM 08006-like) and ^{16}O-poor component, probably water, that was more extensive in the more metamorphosed samples. However, in more fluid dominated systems, such as that which prevailed in the CM parent body (Clayton and Mayeda, 1999; Young et al., 1999), hydrothermal alteration resulted in bulk O isotope variations along slopes that are significantly shallower than the CCAM line. The O isotope variation seen in the COs is similar to that found in the CVs (Greenwood et al., 2010). It is often argued that nebula water O isotopic compositions fell close to ^{16}O-poor extensions of the CCAM or Young and Russell lines (Clayton and Mayeda, 1999; Young et al., 1999; Sakamoto et al., 2007). In this case, to produce the shallower slopes of the bulk CMs in an O three isotope diagram requires some O isotope mass fractionation (e.g., between water and phyllosilicates) and loss of the ^{18}O-poor component (e.g., residual water). The O isotopic variations in the bulk COs and CVs close to the CCAM line are most easily explained if there was little or no loss of residual water, i.e., most or all of the water was consumed by reactions in the CO and CV parent bodies.

Conclusions

Some COs, and related ungrouped chondrites like Acfer 094, are amongst the most primitive chondrites known, as is evident from the high presolar silicate and amorphous silicate abundances in their matrices, and the presence of materials like cosmic symplectite. The chondrules in COs are also unusual in terms of their high plagioclase contents, which makes them particularly attractive targets for Al-Mg dating. COs may also be very similar to the primary anhydrous materials accreted by CM chondrites. Indeed, it is possible that lightly altered CMs could have been misidentified as COs. For all these reasons, identifying the most primitive COs is of considerable scientific interest.

To this end, we have conducted a multi-technique study of 16 Antarctic meteorites that had been classified as primitive COs. This study involved determining: (1) the bulk H, C and N abundances and isotopes, (2) bulk O isotopic compositions, (3) bulk modal mineralogies, and (4) for some selected samples the abundances and compositions of their insoluble organic matter (IOM).

Two of the 16 meteorites do appear to be CMs – BUC 10943 seems to be a fairly typical CM, while MIL 090073 has probably been heated. Of the COs, DOM 08006 is the most primitive based on it bulk and IOM light element geochemistry. It seems to be even more primitive than ALH 77307 (CO3.03), and based on its IOM H/C ratio DOM 08006 experienced a similar thermal history to Semarkona (LL3.00). Hence, we suggest that DOM 08006 be classified as a CO3.00. All but two of the other primitive COs in this study form two groups based on their light element geochemistries. The first group is composed of members of the DOM 08004 pairing group, except DOM 08006. The second group is composed of meteorites belonging to the MIL 03377 and MIL 07099 pairing groups. These two large pairing groups should probably be combined. The two meteorites that do not obviously belong to these groups are heavily weathered.

There is a dichotomy in the bulk O isotopes between the primitive (all Antarctic finds) and the more metamorphosed COs (mostly falls), with more metamorphosed samples lying close to the CCAM line and the primitive compositions being roughly mass fractionated to the low $\delta^{18}O$ side of the CCAM line. EATG leaching experiments indicate that this dichotomy can only partly be explained by the terrestrial weathering experienced by the primitive Antarctic samples. It seems that the more equilibrated samples interacted to a greater extent with ^{16}O-poor material, probably water, than the more primitive meteorites.

Acknowledgements

Ernst Zinner was an exacting mentor and cherished friend to CA for many years, as well as an inspiration to us all.

For supplying the many samples that were necessary for this work, the authors would like to thank: the members of the Meteorite Working Group, Cecilia Satterwhite and Kevin Righter (NASA, Johnson Space Center). US Antarctic meteorite samples are recovered by the Antarctic Search for Meteorites (ANSMET) program, which has been funded by NSF and NASA, and characterized and curated by the Department of Mineral Sciences of the Smithsonian Institution and Astromaterials Curation Office at NASA Johnson Space Center. Reviewers Knut Metzler and Alan Rubin helped significantly improve this manuscript.

CA was partially supported by NASA Cosmochemistry grant NNX14AJ54G. KH was partially supported by NASA Cosmochemistry grant NNX11AG27G. Oxygen isotope studies at the Open University are funded by a Consolidated Grant from the UK Science and Technology Facilities Council (STFC) (Grant Number: ST/L000776/1).

References

Alexander C. M. O. D. (2005) From supernovae to planets: The view from meteorites and IDPs. In: Chondrites and the Protoplanetary Disk (A. N. Krot, E. R. D. Scott and B. Reipurth, eds.), 972-1002.

Alexander C. M. O. D., Bowden R., Fogel M. L. and Howard K. T. (2015) Carbonate abundances and isotopic compositions in chondrites. *Meteoritics Planet. Sci.*, In Press.

Alexander C. M. O. D., Bowden R., Fogel M. L., Howard K. T., Herd C. D. K. and Nittler L. R. (2012) The provenances of asteroids, and their contributions to the volatile inventories of the terrestrial planets. *Science* **337**, 721-723.

Alexander C. M. O. D., Bowden R. and Howard K. (2014) A multi-technique search for the most primitive CO chondrites. *Lunar Planet. Sci.* **45**, #2667.

Alexander C. M. O. D. and Ebel D. S. (2012) Questions, questions: Can the contradictions between the petrologic, isotopic, thermodynamic, and astrophysical constraints on chondrule formation be resolved? *Meteor. Planet. Sci.* **47**, 1157-1175.

Alexander C. M. O. D., Fogel M., Yabuta H. and Cody G. D. (2007) The origin and evolution of chondrites recorded in the elemental and isotopic compositions of their macromolecular organic matter. *Geochim. Cosmochim. Acta* **71**, 4380-4403.

Alexander C. M. O. D., Howard K., Bowden R. and Fogel M. L. (2013) The classification of CM and CR chondrites using bulk H, C and N abundances and isotopic compositions. *Geochim. Cosmochim. Acta* **123**, 244-260.

Alexander C. M. O. D., Newsome S. N., Fogel M. L., Nittler L. R., Busemann H. and Cody G. D. (2010) Deuterium enrichments in chondritic macromolecular material – Implications for the origin and evolution of organics, water and asteroids. *Geochim. Cosmochim. Acta* **74**, 4417-4437.

Bao H. and Koch P. L. (1999) Oxygen isotope fractionation in ferric oxide-water systems: low temperature synthesis. *Geochim. Cosmochim. Acta* **63**, 599-613.

Beaudoin G. and Therrien P. (2009) The updated web stable isotope fractionation calculator. In: Handbook of stable isotope analytical techniques (P. A. DeGroot, ed., 1120-1122.

Bland P. A., Cressey G. and Menzies O. N. (2004) Mineralogy of carbonaceous chondrites by X-ray diffraction and Mössbauer spectroscopy. *Meteor. Planet. Sci.* **39**, 3-16.

Bonal L., Bourot-Denise M., Quirico E., Montagnac G. and Lewin E. (2007) Organic matter and metamorphic history of CO chondrites. *Geochim. Cosmochim. Acta* **71**, 1605-1623.

Brearley A. J. (1993) Matrix and fine-grained rims in the unequilibrated CO3 chondrite, ALHA77307: Origins and evidence for diverse, primitive nebular components. *Geochim. Cosmochim. Acta* **57**, 1521-1550.

Burton A. S., Elsila J. E., Callahan M. P., Martin M. G., Glavin D. P., Johnson N. M. and Dworkin J. P. (2012) A propensity for n-ω-amino acids in thermally altered Antarctic meteorites. *Meteor. Planet. Sci.* **47**, 374-386.

Busemann H., Alexander C. M. O. D. and Nittler L. R. (2007) Characterization of insoluble organic matter in primitive meteorites by microRaman spectroscopy. *Meteor. Planet. Sci.* **42**, 1387-1416.

Chizmadia L. J., Rubin A. E. and Wasson J. T. (2002) Mineralogy and petrology of amoeboid olivine inclusions in CO3 chondrites: Relationship to parent-body aqueous alteration. *Meteor. Planet. Sci.* **37**, 1781-1796.

Choi B. G., Itoh S., Yurimoto H., Rubin A. E., Wasson J. T. and Grossman J. N. (2008) Oxygen-isotopic composition of magnetite in the DOM 03238 CO3.1 chondrite. *Meteor. Planet. Sci. Supp.* **43**, A32.

Clayton R. N. and Mayeda T. K. (1999) Oxygen isotope studies of carbonaceous chondrites. *Geochim. Cosmochim. Acta* **63**, 2089-2104.

Cody G. D., Alexander C. M. O. D., Yabuta H., Kilcoyne A. L. D., Araki T., Ade H., Dera P., Fogel M., Militzer B. and Mysen B. O. (2008) Organic thermometry for chondritic parent bodies. *Earth Planet. Sci. Lett.* **272**, 446-455.

Cressey G. and Schofield P. F. (1996) Rapid whole-pattern profile-stripping method for the quantification of multiphase samples. *Powder Diffraction* **11**, 35-39.

Davidson J., Nittler L. R., Alexander C. M. O. D. and Stroud R. M. (2014a) Petrography of very primitive CO3 chondrites: Dominion Range 08006, Miller Range 07687 and four others. *Lunar Planet. Sci.* **45**, This Vol.

Davidson J., Nittler L. R., Alexander C. M. O. D. and Stroud R. M. (2014b) Petrography of very primitive CO3 chondrites: Dominion Range 08006, Miller Range 07687, and four others. *Lunar Planet. Sci.* **45**, #1384.

Doyle P. M., Jogo K., Nagashima K., Krot A. N., Wakita S., Ciesla F. J. and Hutcheon I. D. (2015) Early aqueous activity on the ordinary and carbonaceous chondrite parent bodies recorded by fayalite. *Nat. Commun.* **6**.

Dunn T. L., Cressey G., McSween H. Y., Jr. and McCoy T. J. (2010) Analysis of ordinary chondrites using powder X-ray diffraction: 1. Modal mineral abundances. *Meteor. Planet. Sci.* **45**, 123-134.

Greenwood R. C. and Franchi I. A. (2004) Alteration and metamorphism of CO3 chondrites: Evidence from oxygen and carbon isotopes. *Meteor. Planet. Sci.* **39**, 1823-1838.

Greenwood R. C., Franchi I. A., Gibson J. M. and Benedix G. K. (2012) Oxygen isotope variation in primitive achondrites: The influence of primordial, asteroidal and terrestrial processes. *Geochim. Cosmochim. Acta* **94**, 146-163.

Greenwood R. C., Franchi I. A., Kearsley A. T. and Alard O. (2010) The relationship between CK and CV chondrites. *Geochim. Cosmochim. Acta* **74**, 1684-1705.

Greenwood R. C., Pearson V. K., Verchovsky A. B., Johnson D., Franchi I. A., Roaldset E., Raade G. and Bartoschewitz R. (2007) The Moss (CO3) meteorite: An integrated isotopic, organic and mineralogical study. *Lunar Planet. Sci.* **38**, #2267.

Grossman J. N. and Brearley A. J. (2005) The onset of metamorphism in ordinary and carbonaceous chondrites. *Meteor. Planet. Sci.* **40**, 87-122.

Hallis L. J., Ishii H. A., Bradley J. P. and Taylor G. J. (2014) Transmission electron microscope analyses of alteration phases in martian meteorite MIL 090032. *Geochim. Cosmochim. Acta* **134**, 275-288.

Hewins R. H., Bourot-Denise M., Zanda B., Leroux H., Barrat J.-A., Humayun M., Göpel C., Greenwood R. C., Franchi I. A., Pont S., Lorand J.-P., Cournède C.,

Gattacceca J., Rochette P., Kuga M., Marrocchi Y. and Marty B. (2014) The Paris meteorite, the least altered CM chondrite so far. *Geochim. Cosmochim. Acta* **124**, 190-222.

Howard K. T., Alexander C. M. O. D., Schrader D. L. and Dyl K. A. (2015) Classification of hydrous meteorites (CR, CM and C2 ungrouped) by phyllosilicate fraction: PSD-XRD modal mineralogy and planetesimal environments. *Geochim. Cosmochim. Acta* **149**, 206-222.

Howard K. T., Benedix G. K., Bland P. A. and Cressey G. (2010) Modal mineralogy of CV3 chondrites by X-ray diffraction (PSD-XRD). *Geochim. Cosmochim. Acta* **74**, 5084-5097.

Howard K. T., Benedix G. K., Bland P. A. and Cressey G. (2011) Modal mineralogy of CM chondrites by X-ray diffraction (PSD-XRD): Part 2. Degree, nature and settings of aqueous alteration. *Geochim. Cosmochim. Acta* **75**, 2735-2751.

Jarosewich E. (1990) Chemical analyses of meteorites: A compilation of stony and iron meteorite analyses. *Meteoritics* **25**, 323-338.

King A. J., Schofield P. F., Howard K. T. and Russell S. S. (2015) Modal mineralogy of CI and CI-like chondrites by X-ray diffraction. *Geochim. Cosmochim. Acta* **165**, 148-160.

Le Guillou C. and Brearley A. (2014) Relationships between organics, water and early stages of aqueous alteration in the pristine CR3.0 chondrite MET 00426. *Geochim. Cosmochim. Acta* **131**, 344-367.

Lee M. R. and Bland P. A. (2004) Mecahnisms of weathering of meteorites recovered from hot an cold deserts and formation of phyllosilicates. *Geochim. Cosmochim. Acta* **68**, 893-916.

Madsen I. C., Scarlett N. V. Y., Cranswick L. M. D. and Lwin T. (2001) Outcomes of the International Union of Crystallography Commission on powder diffraction round robin on quantitative phase analysis: Samples 1a to 1h. *Journal of Applied Crystallography* **34**, 409-426.

Menzies O. N., Bland P. A., Berry F. J. and Cressey G. (2005) A Mössbauer spectroscopy and X-ray diffraction study of ordinary chondrites: Quantification of modal mineralogy and implications for redox conditions during metamorphism. *Meteor. Planet. Sci.* **40**, 1023-1042.

Miller M. F., Franchi I. A., Sexton A. S. and Pillinger C. T. (1999) High precision $\delta^{17}O$ isotope measurements of oxygen from silicates and other oxides: Method and applications. *Rapid Comm. Mass Spec.* **13**, 1211-1217.

Nguyen A. N., Nittler L. R., Stadermann F. J., Stroud R. M. and Alexander C. M. O. D. (2010) Coordinated analyses of presolar grains in the Allan Hills 77307 and Queen Elizabeth Range 99177 meteorites. *Astrophys. J.* **719**, 166-189.

Nguyen A. N., Stadermann F. J., Zinner E., Stroud R. M., Alexander C. M. O. D. and Nittler L. R. (2007) Characterization of presolar silicate and oxide grains in primitive carbonaceous chondrites. *Astrophys. J.* **656**, 1223-1240.

Nguyen A. N. and Zinner E. (2004) Discovery of presolar silicate grains in the Acfer 094 carbonaceous chondrite. *Science* **303**, 1496-1499.

Nittler L. R., Alexander C. M. O. D. and Stroud R. M. (2013) High abundance of presolar materials in CO3 chondrite Dominion Range 08006. *Lunar Planet. Sci.* **44**, #2367.

Quirico E., Raynal P. I. and Bourot-Denise M. (2003) Metamorphic grade of organic matter in six unequilibrated ordinary chondrites. *Meteor. Planet. Sci.* **38**, 795-811.

Sakamoto N., Seto Y., Itoh S., Kuramoto K., Fujino K., Nagashima K., Krot A. N. and Yurimoto H. (2007) Remnants of the early Solar System water enriched in heavy oxygen isotopes. *Science* **317**, 231-233.

Savin S. M. and Lee M. (1988) Isotopic studies of phyllosilicates. In: Hydrous phyllosilicates (exclusive of micas) (S. W. Bailey, ed., 189-223.

Schrader D. L., Davidson J., Greenwood R. C., Franchi I. A. and Gibson J. M. (2014) A water–ice rich minor body from the early Solar System: The CR chondrite parent asteroid. *Earth Planet. Sci. Lett.* **407**, 48-60.

Schrader D. L., Franchi I. A., Connolly Jr H. C., Greenwood R. C., Lauretta D. S. and Gibson J. M. (2011) The formation and alteration of the Renazzo-like carbonaceous chondrites I: Implications of bulk-oxygen isotopic composition. *Geochim. Cosmochim. Acta* **75**, 308-325.

Schultz L. (1986) Allende in Antarctia: Temperatures in Antarctic meteorites. *Meteoritics* **21**, 505.

Seto Y., Sakamoto N., Fujino K., Kaito T., Oikawa T. and Yurimoto H. (2008) Mineralogical characterization of a unique material having heavy oxygen isotope anomaly in matrix of the primitive carbonaceous chondrite Acfer 094. *Geochim. Cosmochim. Acta* **72**, 2723-2734.

Sheppard S. M. F. and Gilg H. A. (1996) Stable isotope geochemistry of clay minerals. *Clay Minerals* **31**, 1-24.

Smith J. W. and Kaplan I. R. (1970) Endogenous carbon in carbonaceous meteorites. *Science* **167**, 1367-1370.

Starkey N. A., Jackson C. R. M., Greenwood R. C., Parman S., Franchi I. A., Jackson M., Fitton J. G., Stuart F. M., Kurz M. and Larsen L. M. (2016) Triple oxygen isotopic composition of the high-3He/4He mantle. *Geochim. Cosmochim. Acta* **176**, 227-238.

Tenner T. J., Nakashima D., Ushikubo T., Kita N. T. and Weisberg M. K. (2015) Oxygen isotope ratios of FeO-poor chondrules in CR3 chondrites: Influence of dust enrichment and H_2O during chondrule formation. *Geochim. Cosmochim. Acta* **148**, 228-250.

Ushikubo T., Kimura M., Kita N. T. and Valley J. W. (2012) Primordial oxygen isotope reservoirs of the solar nebula recorded in chondrules in Acfer 094 carbonaceous chondrite. *Geochim. Cosmochim. Acta* **90**, 242-264.

Ushikubo T., Nakashima D., Kimura M., Tenner T. J. and Kita N. T. (2013) Contemporaneous formation of chondrules in distinct oxygen isotope reservoirs. *Geochim. Cosmochim. Acta* **109**, 280-295.

Vollmer C., Hoppe P., Stadermann F. J., Floss C. and Brenker F. E. (2009) NanoSIMS analysis and Auger electron spectroscopy of silicate and oxide stardust from the carbonaceous chondrite Acfer 094. *Geochim. Cosmochim. Acta* **73**, 7127-7149.

Yan M., Li Y., Hammer C. U., Gundestrup N. S., Tan D., Wen J., Wang D., Sun B., Kang J. and Liu L. (2002) Oxygen isotope composition of surface snow collected along the traverse route from Zhongshan Station toward Dome A, Antarctica. *Polar Meteorology and Glaciology* **16**, 133-139.

Young E. D., Ash R. D., England P. and Rumble D., III (1999) Fluid flow in chondritic parent bodies: Deciphering the compositions of planetesimals. *Science* **286**, 1331-1335.

Young E. D. and Russell S. S. (1998) Oxygen reservoirs in the early solar nebula inferred from an Allende CAI. *Science* **282**, 452-455.

Zheng Y.-F. (1993) Calculation of oxygen isotope fractionation in hydroxyl-bearing silicates. *Earth Planet. Sci. Lett.* **120**, 247-263.

Figure Captions.

Figure 1. The bulk H contents and H isotopic compositions of the primitive Antarctic COs analyzed in this study. The samples have been given different symbols according to their weathering grade (A-C). There appear to be two trends in the data reflecting Antarctic weathering of COs with two distinct initial compositions. Most samples form a linear trend with the most weathered CO being MIL 090785. The two most primitive COs, DOM 08006 and ALH 77307, form a separate trend that roughly passes through the composition of MIL 090785.

Figure 2. The O isotopic compositions of CO falls and finds. The colored symbols are from this study. The grey symbols from previously published Open University CO analyses (Greenwood and Franchi, 2004; Greenwood et al., 2007). TFL is the terrestrial fractionation line. CCAM is the carbonaceous chondrite anhydrous minerals line (Clayton and Mayeda, 1999). The blue solid line, labeled (1), is the best-fit line through the CO falls (data for this study only) and the untreated Antarctic Finds (data for this study only, but excluding MIL 090785). This line has a slope of 0.52 and is, therefore, essentially identical in slope to a mass fractionation line. The grey arrow, labeled (2), is the tie line joining the CO falls (data for this study only) with SLAP (Standard Light Antarctic Precipitation, $\delta^{17}O$ = -28.9 ‰, $\delta^{18}O$= -55.5 ‰). This tie line has a slope of 0.43. Also shown are the isotopic compositions after leaching the bulk powders with EATG. Tie lines connect previously analyzed samples with their compositions after leaching. Most samples move down towards the CCAM line after EATG leaching. However, note the very large shift in $\delta^{18}O$ exhibited by the heavily weathered MIL 090785.

Figure 3. Comparison of the O isotopic compositions of bulk and EATG-leached CO falls. Symbols: F – Felix; K – Kainsaz; L – Lance; M – Moss; Or – Ornans; W – Warrenton; See text for further discussion.

Figure 4. The O isotope compositions of CO falls and finds shown in relation to various reference lines. Murchison anhydrous minerals composition point is based on analysis of

mineral separates by Clayton and Mayeda (1999). Abbreviations: Y&R – Young & Russell line (Young and Russell, 1998); PCM - Primitive Chondrule Minerals line (Ushikubo et al., 2012; Tenner et al., 2015); CCAM – Carbonaceous Chondrite Anhydrous Minerals line (Clayton and Mayeda, 1999).

Figure 5. The likely O isotope fractionation effects on bulk samples resulting from Antarctic weathering. The tie lines join the composition of Kainsaz, the lowest metamorphic grade CO fall, to the compositions for akaganeite and smectite in equilibrium with water having a SLAP-like isotopic composition at 0°C. While only two mineral compositions are shown these define the range of alteration phases found in weathered Antarctic meteorites. Thus, the alteration products formed by weathering in Antarctica will plot along the terrestrial fractionation line (TFL) between these two end-members. A = akaganeite, S = smectite. For clarity, analyses of the EATG-treated residues for Colony, ALH 82101 and MIL 090785 (Table 3, Fig. 2) have not been plotted on this diagram.

Figure 6. A diagram showing how changes in the $\delta^{18}O$ values of Antarctic water will affect the $\delta^{18}O$ values of the secondary mineral assemblage. Abbreviations as in Figure 5 (see text for further discussion).

Table 1. The bulk C abundances and isotopic compositions of the COs analyzed. They are divided into groups based on the similarity of their C abundances and isotopic compositions.

Meteorite	Weath.	Pairing	C (wt.%)	$\delta^{13}C$ (‰)	H (wt.%)	δD (‰)	N (wt.%)	$\delta^{15}N$ (‰)
DOM 08006[1]	A/B	DOM 08004	1.19	-5.0	0.439±0.005	4.7±4.8	0.019	6.5
DOM 08006b	A/B	DOM 08004	1.20	-4.2	0.476±0.004	-4.7±0.8	0.026	8.6
ALH 77307[2]	*Ae*		*0.84*	*-7.1*	*0.546±0.010*	*-48.2±4.4*	*0.025*	*-2.7*
Group 1								
DOM 03238	B		0.90	-11.9	0.300±0.001	-73.1±0.4	0.035	-6.0
DOM 08004	B	DOM 08004	0.91	-11.3	0.332±0.001	-89.8±3.8	0.031	-7.9
DOM 10104	A/B	DOM 08004	0.88	-11.7	0.398±0.002	-98.7±1.3	0.072	-5.9
Group 2								
MIL 03377	B	MIL 03377	0.64	-7.3	0.385±0.002	-92.9±0.3	0.032	-5.5
MIL 05013[1]	B/Ce	MIL 03377	0.65	-7.1	0.292±0.029	-73.7±0.2	0.010	-7.2
MIL 05013b	B/Ce	MIL 03377	0.64	-7.2	0.316±0.003	-90.5±2.0	0.018	-4.0
MIL 05024	A/B	MIL 03377	0.64	-7.6	0.352±0.001	-89.7±3.2	0.032	-7.8
MIL 07182	B	MIL 07099	0.66	-7.0	0.332±0.004	-85.5±1.2	0.027	-8.5
MIL 07193	A	MIL 07099	0.63	-7.6	0.365±0.005	-85.8±3.8	0.030	-8.4
MIL 07709	B	MIL 07099	0.62	-7.0	0.311±0.002	-85.4±0.3	0.021	-8.1
MIL 090010	A/B	MIL 07099	0.69	-6.5	0.374±0.001	-94.0±0.1	0.016	-4.9
MIL 090038	B	MIL 07099	0.64	-7.2	0.339±0.005	-83.9±3.1	0.035	-3.3
MIL 03442	C	MIL 03377	0.47	-6.7	0.470±0.006	-116.5±1.6	0.018	-8.5
MIL 090785	C	MIL 07099	0.09	0.3	0.780±0.002	-178.1±3.0	0.015	13.9
CM								
BUC 10943	B		1.52	-7.6	1.217±0.004	-109.1±2.6	0.095	15.0
MIL 090073	B/C	MIL 07099	0.72	-14.7	0.598±0.001	-136.0±0.5	0.047	10.5

[1]These samples were from the study of Burton et al. (2012).
[2]From Alexander et al. (2012).

Table 2. The wt.% C in IOM isolated from the selected samples, along with the elemental and isotopic compositions of the IOM.

	C (wt.%)	$\delta^{13}C$ (‰)	H/C (at.)	δD (‰)	N/C (at.)	$\delta^{15}N$ (‰)
Semarkona[1]	*0.36*	*-23.7*	*0.476*	*2322*	*0.0149*	*26.9*
DOM 08006	0.91	-6.7	0.465±0.002	476±15	0.0169	10.2
ALH 77307[1]	*0.48*	*-8.3*	*0.301*	*340*	*0.0204*	*3.0*
Group 1						
DOM 03238	0.42	-10.4	0.276±0.001	528±11	0.0124	0.2
DOM 10104	0.64	-11.2	0.320±0.001	435±11	0.0158	-6.3
Group 2						
MIL 05013	0.47	-8.7	0.220	912	0.0144	-3.9
MIL 090010	0.32	-8.1	0.220±0.001	893±4	0.0154	-2.2
CM						
BUC 10943	0.57	-18.5	0.645±0.004	773±18	0.0335	-4.2
MIL 090073	0.49	-16.7	n.d.		0.0277	21.6

[1]From Alexander et al. (2007).

Table 3. The O isotopic compositions of bulk and EATG-leached samples.

SAMPLE	N	$\delta^{17}O$ (‰)	1σ	$\delta^{18}O$ (‰)	1σ	$\Delta^{17}O$ (‰)	1σ
Antarctic COs							
DOM 08006	4	-7.60	0.23	-4.83	0.14	-5.08	0.16
Group 1							
DOM 08004	3	-6.89	0.27	-4.14	0.23	-4.74	0.16
DOM 10104	2	-6.90	0.19	-4.43	0.30	-4.60	0.03
Group 2							
MIL 03377	2	-7.41	0.03	-5.22	0.07	-4.70	0.01
MIL 05013	2	-7.65	0.04	-5.35	0.05	-4.87	0.01
MIL 05024	2	-7.80	0.21	-5.46	0.25	-4.96	0.08
MIL 07182	2	-7.26	0.01	-4.80	0.01	-4.76	0.01
MIL 07193	2	-7.61	0.05	-5.36	0.03	-4.83	0.03
MIL 07709	2	-7.54	0.01	-4.92	0.04	-4.98	0.01
MIL 090010	2	-7.26	0.34	-4.73	0.59	-4.80	0.03
MIL 090038	1	-7.39		-4.92		-4.83	
MIL 03442	1	-7.67		-5.98		-4.56	
MIL 090785	2	-8.87	0.36	-9.36	0.53	-4.00	0.09
CO Falls							
Felix	2	-5.84	0.08	-2.01	0.12	-4.80	0.01
Kainsaz	2	-6.60	0.03	-2.61	0.00	-5.24	0.03
Lance	2	-5.75	0.06	-2.00	0.08	-4.71	0.02
Moss	2	-5.94	0.05	-2.06	0.02	-4.87	0.04
Ornans	2	-5.39	0.12	-1.56	0.14	-4.58	0.05
Warrenton	2	-6.12	0.03	-2.36	0.02	-4.89	0.02
CM							
MIL 090073	2	-1.27	0.03	4.50	0.03	-3.61	0.01
EATG-leached CO finds							
ALH 77307	2	-7.52	0.08	-3.90	0.02	-5.49	0.07
ALH 82101	1	-5.81		-1.97		-4.79	
Colony	2	-5.22	0.07	-2.02	0.13	-4.17	0.00
DOM 08004	1	-7.78		-4.31		-5.54	
DOM 08006	2	-8.49	0.21	-5.21	0.23	-5.77	0.09
MIL 03442	2	-8.08	0.15	-4.70	0.20	-5.64	0.05
MIL 05024	4	-7.84	0.07	-4.48	0.09	-5.51	0.05
MIL 090038	2	-7.87	0.41	-4.46	0.47	-5.55	0.16
MIL 090785	3	-6.25	1.09	-0.86	1.53	-5.80	0.34

CO falls							
Lance	2	-6.20	0.01	-2.46	0.13	-4.92	0.06
Ornans	2	-6.23	0.14	-2.46	0.11	-4.95	0.08
Warrenton	2	-6.77	0.00	-3.23	0.03	-5.09	0.02

Table 4. Volume percents of minerals as determined by PSD-XRD.

Sample	Fo_{100}	Fo_{90}	Fo_{80}	Fo_{60}	Fo_{40}	En	Sulf.	Metal	Magn.	Chro.	Phyll.	Amor.
DOM 08006	41			10		22	3	1	6		2	15
ALH 77307		20		17		28	2	2	8		4	20
Group 1												
DOM 08004		28		15		26	3	1	6		3	18
DOM 10104		28		16		23	2		5		3	22
Group 2												
MIL 03377	36			11		26	3	2	6		2	15
MIL 05013		24		15		27	3		6		1	24
MIL 05024	38			17		20	3	2	5		2	13
MIL 07182	36			12		19	2	1	4		1	25
MIL 07193	30			13		23	3	2	4		3	23
MIL 07709	37			11		24	2	2	5		1	19
MIL 090010	26		16		2	23	2	1	7		1	21
MIL 090038	36			14		23	2		5		4	16
MIL 03442	33			11		22	3	1	5		1	25
Felix		40			16	27	3	2	3	1		
CM												
BUC 10943[1]		5	2			15	3		2		69	
MIL 090073		28		10		24	3		3		1	31

Abreviations: Fo – forsterite; En – enstatite; Sulf. – iron sulfides; Magn. – magnetite; Chro. - chromite; Phyll. – phyllosilicates; Amor. – Fe-bearing amorphous material.

[1]Gypsum (3 vol.%) and calcite (1 vol.%) were also detected in BUC 10943.

Table 5. The estimated concentrations and isotopic compositions of H in water/OH after subtracting the organic components assuming that the bulk C in the samples are entirely in organic material with H/C ratios and δD values like that of the extracted IOM (Table 2).

	H (wt.%)	δD (‰)
DOM 08006	0.43	-57
ALH 77307	0.52	-64
Group 1		
DOM 03238	0.28	-118
DOM 10104	0.37	-132
Group 2		
MIL 05013	0.30	-129
MIL 090010	0.36	-129

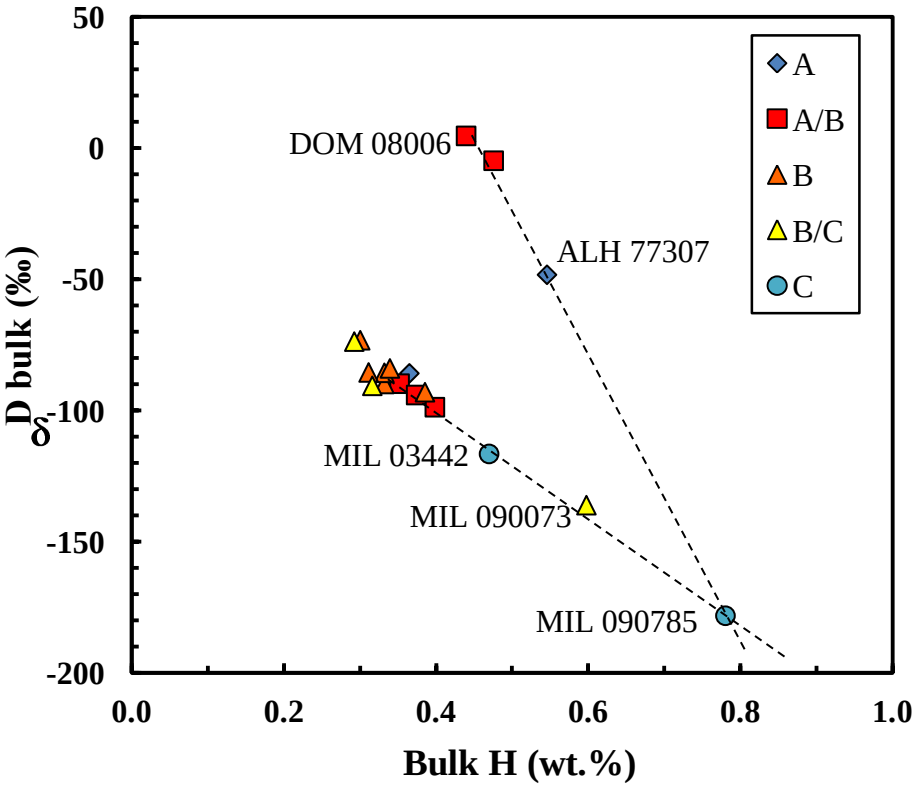

Figure 1.

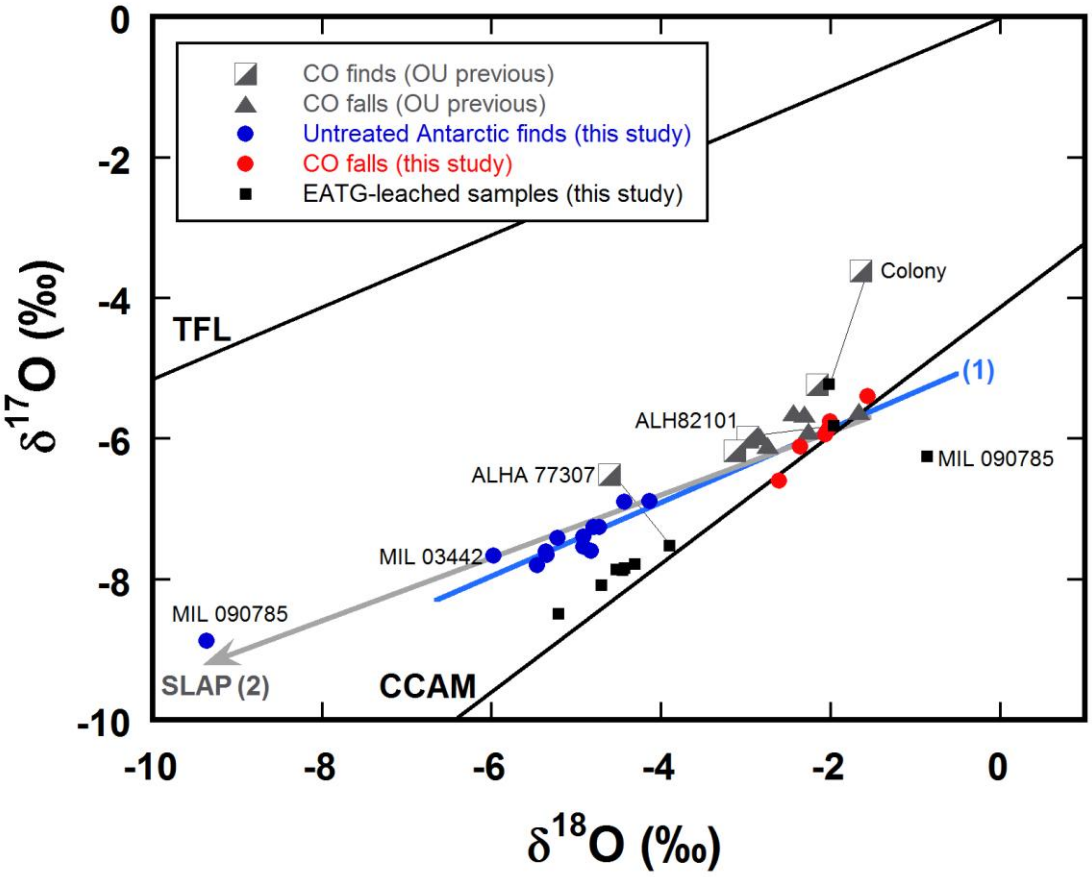

Figure 2.

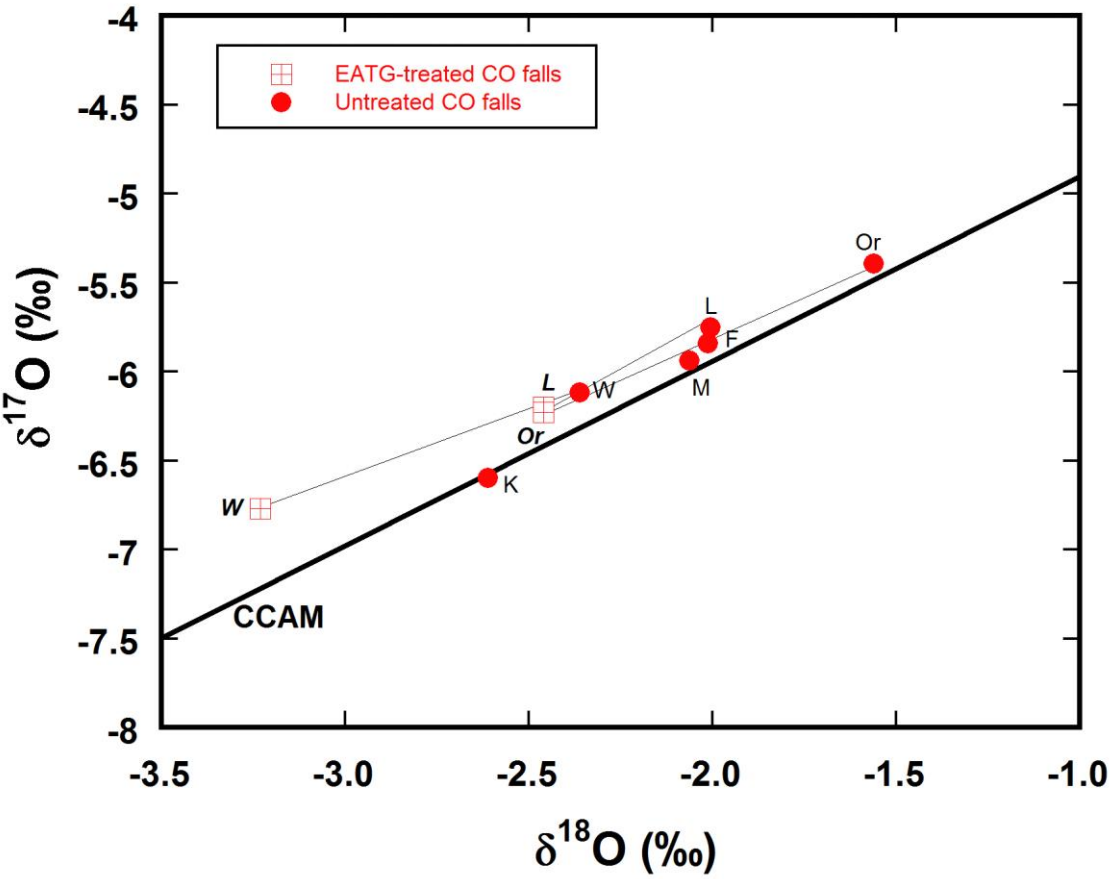

Figure 3.

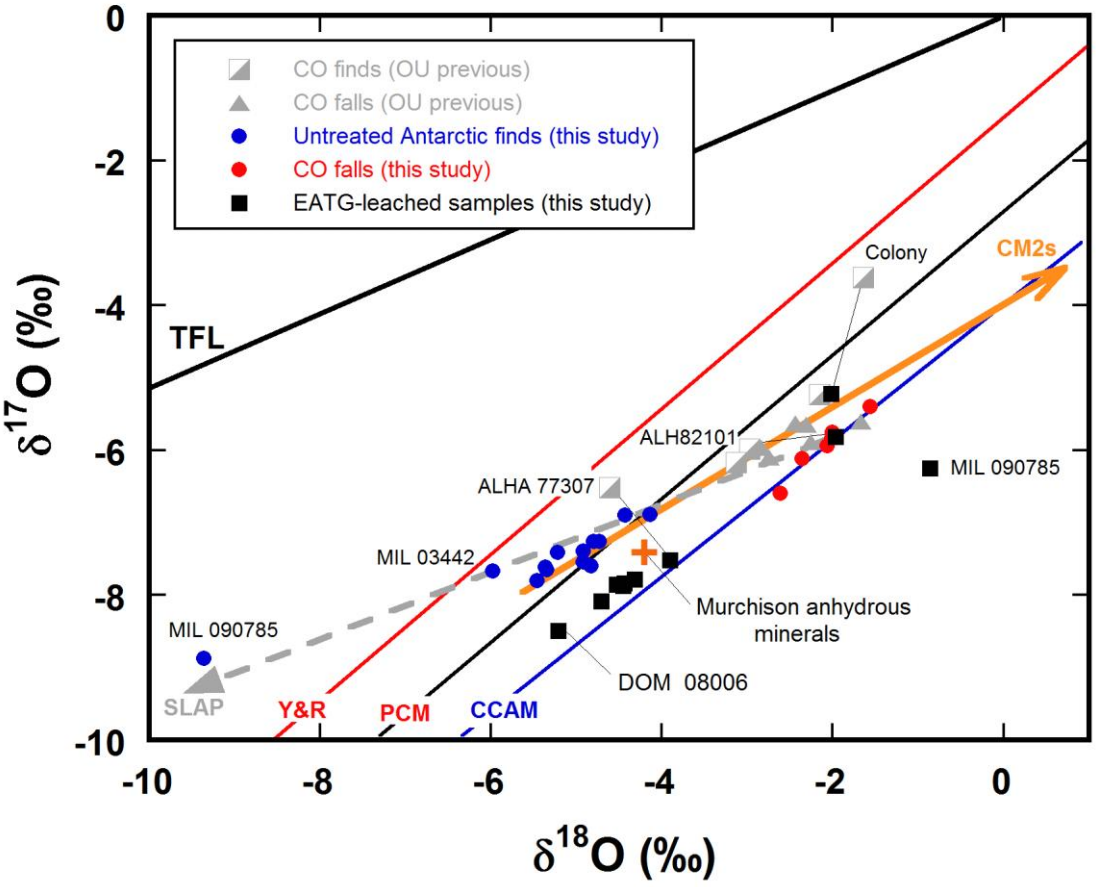

Figure 4.

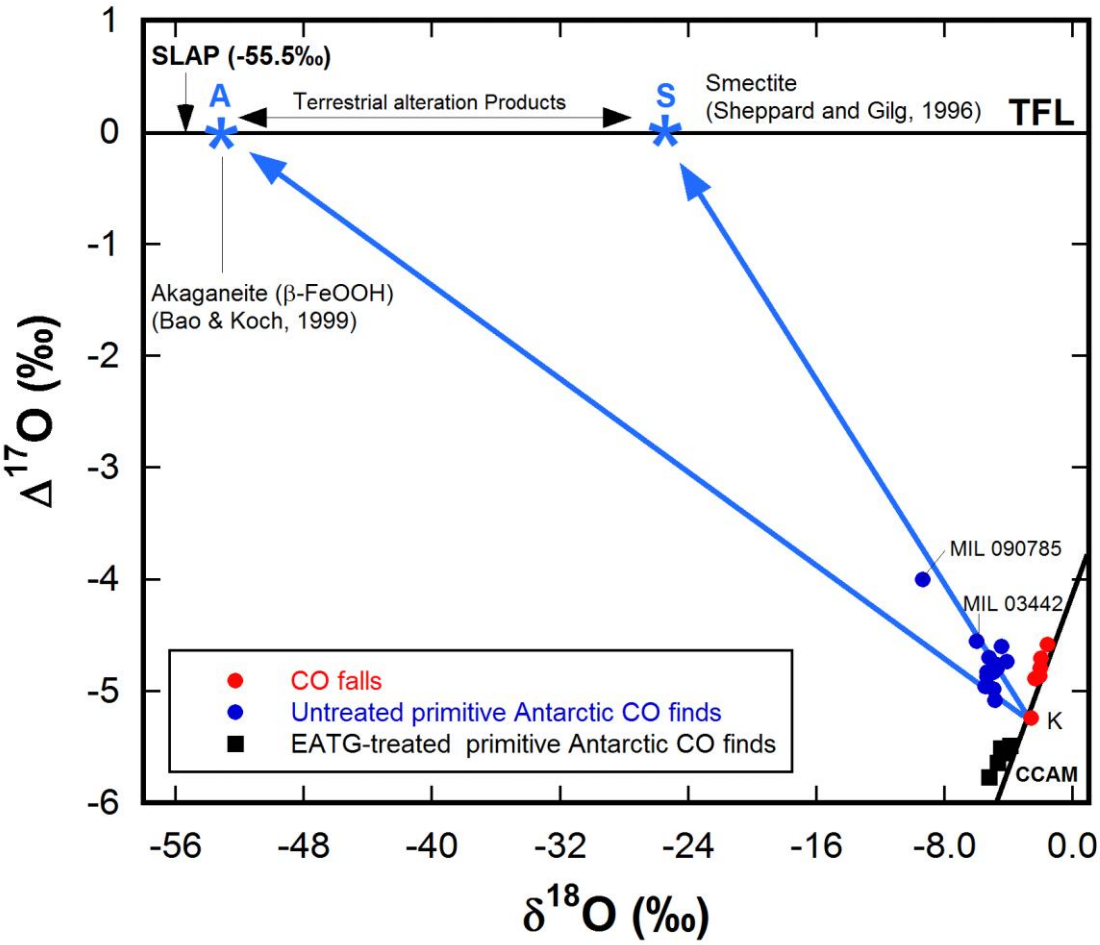

Figure 5.

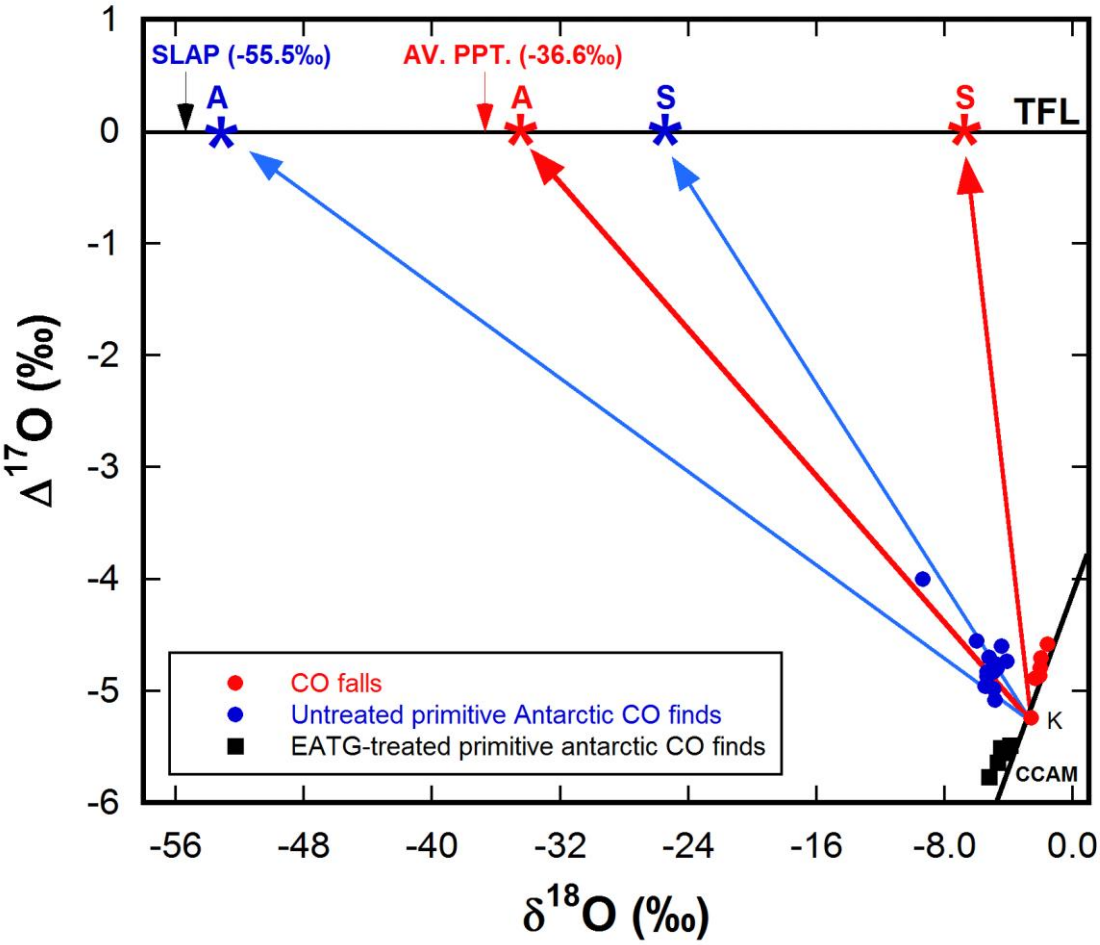

Figure 6.